



**HAL**  
open science

## Estimation of vehicle's vertical and lateral tire forces considering road angle and road irregularity

Kun Jiang, Adina Pavelescu, Alessandro Correa Victorino, Ali Charara

► **To cite this version:**

Kun Jiang, Adina Pavelescu, Alessandro Correa Victorino, Ali Charara. Estimation of vehicle's vertical and lateral tire forces considering road angle and road irregularity. 17th International IEEE Conference on Intelligent Transportation Systems (ITSC 2014), Oct 2014, Qingdao, China. pp.342-347, 10.1109/ITSC.2014.6957714 . hal-01088574

**HAL Id: hal-01088574**

**<https://hal.science/hal-01088574>**

Submitted on 21 Apr 2016

**HAL** is a multi-disciplinary open access archive for the deposit and dissemination of scientific research documents, whether they are published or not. The documents may come from teaching and research institutions in France or abroad, or from public or private research centers.

L'archive ouverte pluridisciplinaire **HAL**, est destinée au dépôt et à la diffusion de documents scientifiques de niveau recherche, publiés ou non, émanant des établissements d'enseignement et de recherche français ou étrangers, des laboratoires publics ou privés.

# Estimation of vehicle's vertical and lateral tire forces considering road angle and road irregularity

Kun Jiang, Adina Pavelescu, Alessandro Victorino, Ali Charara

**Abstract**— Vehicle dynamics is an essential topic in development of safety driving systems. These complex and integrated control units require precise information about vehicle dynamics, especially, tire/road contact forces. Nevertheless, it is lacking an effective and low-cost sensor to measure them directly. Therefore, this study presents a new method to estimate these parameters by using observer technologies and low-cost sensors which are available on the passenger cars in real environment. In our previous work, observers have been designed to estimate the vehicle tire/road contact forces and sideslip angles. However, the previous study just considered the situation of the vehicles running on a level road. In our recent study, vehicle mathematical models are reconstructed to suit banked road and inclined road. Then, Kalman Filter is used to improve the estimation of vehicle dynamics. Finally, the estimator is tested both on simulation CALLAS and on the experimental vehicle DYNA.

## I. INTRODUCTION

The advanced driver assistance system is designed to increase car safety and more generally road safety. Except for some passive safety systems, for example the seat belts, airbags, another approach proposed as active safety system can also effectively help avoid accidents. To prevent accidents actively, it is necessary to measure vehicle dynamics, which allow the assessment of the dangerousness of the driving situation. However, the states of vehicle dynamics such as the tire contact forces, sideslip angles are very difficult to measure directly. In addition, these sensors are very expensive or in-existent to install in ordinary cars. This leads to the need and effort given in the development of state observer applied to the estimation of these parameters.

Vehicle dynamic estimation has been studied by many researchers. For example, in [7], the vertical tire forces are calculated by a 14 Degree of Freedom vehicle model. More recently, the vertical and lateral forces at each tire have been estimated in [4] and [5]. However, these studies are under the hypothesis that the vehicle is running on a leveled road. In reality, the environment may include difficult features such as undulating terrain, and deformable surfaces.

The main contribution of this study is to rebuild the vertical force estimators in order to take into account the roll angle, pitch angle and road angle.

To evaluate the performance of our observers, the vehicle simulation software PROSPER/CALLAS [4] is used. After the Chicane simulation tests, we have evaluated our new observer with the experimental vehicle DYNA, a Peugeot 308.

The authors are with Heudiasyc, CNRS UMR 7253, Université de Technologie de Compiègne, 60205, France. kun.jiang@hds.utc.fr, apaveles@etu.utc.fr, acorreau@hds.utc.fr, acharara@hds.utc.fr

DYNA is equipped with sensors which are able to measure in real time the parameters used in the implementation of our observers as shown in the Figure 1.

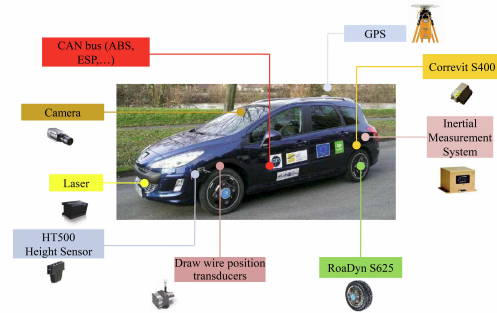


Fig. 1. Experimental vehicle: DYNA

This paper is organized as follows. Section 2 presents the vehicle models that have been reconstructed. Section 3 describes how the observer is constructed. Then, experiment is conducted in Section 4. Finally, concluding remarks and future perspectives are given in Section 5.

## II. VEHICLE MODELING

Many mathematical models have been proposed for the vehicle dynamics description. However, the analytical approach is limited to the existence of large numbers of components, subsystems. The embedded systems usually can't afford much computation ability. Thus, we need to simplify the vehicle modeling with reasonable assumption in order to find the mathematical solutions and satisfy our requirement of computational power. The vehicle dynamics models we used can be classified in three parts as shown in Figure 2.

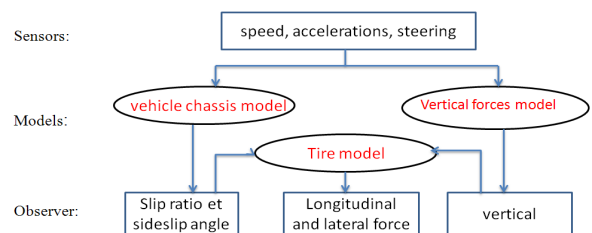


Fig. 2. Structure of complete vehicle model

The study here is to propose a new vertical forces model, which considers roll angle, pitch angle and road irregularity. Then we have combined our vertical model with the existent lateral dynamics model [1] to build a new observer of vehicle dynamics, observing vertical and lateral tire forces.

#### A. Acceleration Measurement in dynamic situation

In the previous vertical force model, the wheel load shifts because of the acceleration variation[5].

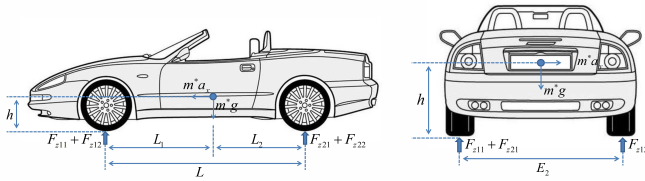


Fig. 3. Vertical load distribution

The model of vertical load distribution is shown as below:

$$F_{z11} = \frac{1}{2}m\left(\frac{L_2}{L} - \frac{a_x h}{gL}\right)g - m\left(\frac{L_2}{L} - \frac{a_x h}{gL}\right)\frac{a_y h}{E_1} \quad (1)$$

where L is the wheel base,  $L = L_1 + L_2$ , h is the height of center of gravity,  $E_{1,2}$  are the vehicle's track(front,rear).

In the previous study, the car is considered as running on a level road so that the force of gravity acts only in the direction vertical to the vehicle. This assumption simplified the measurement of accelerations.

In our recent study, we try to provide a general vertical force model that is suitable for all road geometry. We proposed to distinguish the accelerations caused by the vehicle's motion from the gravitational acceleration. In this way, the influences of the road angle and road irregularity are considered.

In irregular road situation, the measured accelerations contain two parts, one is caused by motion,  $a_{xmot}$ ,  $a_{ymot}$ ,  $a_{zmot}$ , and the other is caused by gravity,  $a_{xgra}$ ,  $a_{ygra}$ ,  $a_{zgra}$ .

To simplify the calculation of vertical forces, we can transform the irregular road situation into the equivalent level road situation. The equivalent accelerations are:

$$\begin{aligned} a_{xequ} &= a_{xmot} + a_{xgra} \\ a_{yequ} &= a_{ymot} + a_{ygra} \\ a_{zequ} &= -a_{zmot} + a_{zgra} \end{aligned} \quad (2)$$

Then according to the load transfer theory, the equation of vertical force is changed to:

$$F_{z11} = \frac{1}{2}m\left(\frac{L_2}{L} - \frac{a_{xequ}h}{a_{zequ}L}\right)a_{zequ} - m\left(\frac{L_2}{L} - \frac{a_{xequ}h}{a_{zequ}L}\right)\frac{a_{yequ}h}{E_1} \quad (3)$$

The accelerometer measures directly the sum of accelerations caused by the vehicle's motion and by gravity. However, the measured quantity is influenced by the pitch and roll angle. The coordinate of accelerometer should be rotated to be parallel to the road.

As a result, the equivalent accelerations can be calculated by the measured accelerations as follow:

$$\begin{pmatrix} a_{xequ} \\ a_{yequ} \\ a_{zequ} \end{pmatrix} = R_\theta R_\phi \begin{pmatrix} a_{xzm} \\ a_{yzm} \\ a_{zsm} \end{pmatrix} \quad (4)$$

Where the rotation matrices are :

$$R_\theta = \begin{pmatrix} 1 & 0 & 0 \\ 0 & \cos \theta_v & -\sin \theta_v \\ 0 & \sin \theta_v & \cos \theta_v \end{pmatrix}, R_\phi = \begin{pmatrix} \cos \phi_v & 0 & \sin \phi_v \\ 0 & 1 & 0 \\ -\sin \phi_v & 0 & \cos \phi_v \end{pmatrix} \quad (5)$$

where  $\theta_v$  and  $\phi_v$  are the pitch angle and roll of the vehicle chassis.  $a_{xzm}$ ,  $a_{yzm}$ ,  $a_{zsm}$  are the measured accelerations by the accelerometer installed at the chassis.

After the rotation of the measured accelerations, we can transform the irregular road condition into the equivalent level road condition.

#### B. Roll and Pitch Dynamics

The equation (3) already provides a general mathematical model of vertical forces for all road geometry. However, the roll and pitch dynamics are not directly appeared in this model. The model doesn't consider the movement of suspension systems. In a dynamic driving situation, like braking, turning, or at irregular road, the suspension system will greatly change the vehicle dynamics.

In order to reduce the number of parameters in the model, we simplify the suspension system with a parallel spring and damper as shown in the Figure 4. We combine the suspension and tire into one system, in which  $K_r$  is the equivalent total rotational stiffness and  $C_r$  is the equivalent total damping coefficient.

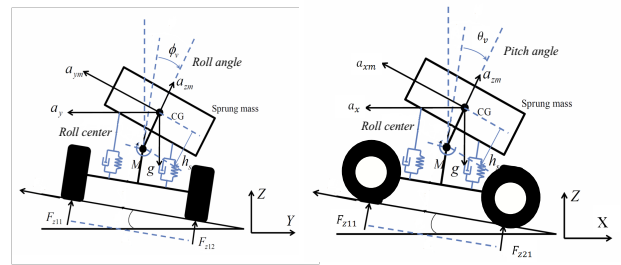


Fig. 4. Roll dynamics and pitch dynamics

Usually, the roll center changes according to the vehicle movement that defects on the suspension deflection, here we assumed that the vehicle roll center keeps constant and its distance with the center of gravity is noted as  $h_s$ . According to the torque balance in the roll axis, the roll dynamics of the vehicle body can be described by the following differential equation:

$$\begin{aligned} I_{xx}\ddot{\phi}_v &= -C_r\dot{\phi}_v - K_r\phi_v + m_v h_s a_{ym} \\ I_{yy}\ddot{\theta}_v &= -C_r\dot{\theta}_v - K_r\theta_v + m_v h_s a_{xm} \end{aligned} \quad (6)$$

Where  $I_{xx}$  is the moment of inertia of the vehicle with respect to the roll axis,  $I_{yy}$  is respect to the pitch axis and  $h_s$  is the height of the sprung mass about the roll axis.

### C. Roll and Pitch Angle Calculation

The roll angle can be calculated by integrating the roll rate measured by accelerometer. However, the sensor bias will also be integrated, which causes large calculation error. Hac [11] proposes a roll angle model expressed with suspension deflection, with which the pitch dynamics affection is decoupled from the roll motion. In this study, the roll angle and pitch angle is obtained via suspension deflection sensors.

$$\phi_v = \frac{\Delta_{11} - \Delta_{12} + \Delta_{21} - \Delta_{22}}{2E}, \quad \theta_v = \frac{\Delta_{11} + \Delta_{12} - \Delta_{21} - \Delta_{22}}{2(L_1 + L_2)} + \theta_s \quad (7)$$

where  $\Delta_{ij}$  is measured suspension deflection at each wheel of the vehicle and E denotes the effective track's width,  $\theta_s$  is the inclination angle at static state.

### D. Vertical Forces Calculation

In the previous vertical force model, the load transfer is caused by the longitudinal and lateral accelerations. In our recent study, we suppose that the load transfer are regarded as caused by the torque of suspension systems.

In the case of roll movement, the torque of suspension is denoted as  $M_\phi$ . Then according to the torque balance, we have:

$$\begin{aligned} F_{z1} + F_{z2} &= m_v a_{zequ} \\ F_{z1} L_1 - F_{z2} L_2 &= M_\phi \end{aligned} \quad (8)$$

Where  $F_{zij}$  ( $i, j = 1, 2$ ) is the vertical force of each wheel,  $i = 1$  means front axle,  $j = 1$  means left side.  $F_{z1}$  is the total vertical force of front axle.

In the case of pitch movement, the torque of suspension is denoted as  $M_\theta$ . In the same way, we have:

$$\begin{aligned} F_{z1} &= F_{z11} + F_{z12} \\ F_{z11} \frac{E_1}{2} - F_{z12} \frac{E_1}{2} &= M_\theta \left( \frac{F_{z1}}{F_{z1} + F_{z2}} \right) \\ F_{z21} \frac{E_2}{2} - F_{z22} \frac{E_2}{2} &= M_\theta \left( \frac{F_{z2}}{F_{z1} + F_{z2}} \right) \end{aligned} \quad (9)$$

In the moment with both pitch and roll movement, the torque of the suspension systems can be calculated by the following equations:

$$\begin{aligned} M_\phi &= K_r \phi + C_r \dot{\phi} \\ M_\theta &= K_r \theta + C_r \dot{\theta} \end{aligned} \quad (10)$$

With all the equations above, vertical force at four wheels can be approximately formulated as:

$$\begin{aligned} F_{z11} &= \frac{m_v L_2 a_{zequ}}{2L} - \frac{L_2 (K_r \theta + C_r \dot{\theta})}{LE_1} + \frac{K_r \phi + C_r \dot{\phi}}{2L} - \frac{M_\theta M_\phi}{m_v a_{zr} LE_1} \\ F_{z12} &= \frac{m_v L_2 a_{zequ}}{2L} + \frac{L_2 (K_r \theta + C_r \dot{\theta})}{LE_1} + \frac{K_r \phi + C_r \dot{\phi}}{2L} + \frac{M_\theta M_\phi}{m_v a_{zr} LE_1} \\ F_{z21} &= \frac{m_v L_1 a_{zequ}}{2L} - \frac{L_1 (K_r \theta + C_r \dot{\theta})}{LE_2} - \frac{K_r \phi + C_r \dot{\phi}}{2L} + \frac{M_\theta M_\phi}{m_v a_{zr} LE_2} \\ F_{z22} &= \frac{m_v L_1 a_{zequ}}{2L} + \frac{L_1 (K_r \theta + C_r \dot{\theta})}{LE_2} - \frac{K_r \phi + C_r \dot{\phi}}{2L} - \frac{M_\theta M_\phi}{m_v a_{zr} LE_2} \end{aligned} \quad (11)$$

In the final model equations, the pitch and roll angle are directly used to present the roll and pitch dynamics. It is more suitable to dynamic driving situations at irregular roads. However, it is limited due to the variation of certain parameters and assumptions that aimed at simplifying the model. Consequently, in the next section, the observer technique is introduced to improve the estimation.

## III. OBSERVER DESIGN

The overall calculation process of the observer can be expressed by the Figure 5:

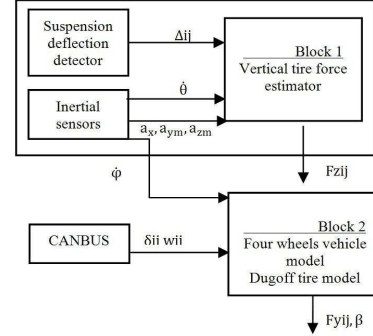


Fig. 5. Observer structure

The first block provides the vertical tire forces for the calculation of lateral dynamics in the second block, which is already realized in our previous work[1], [2], [3]. Our study here is to modify the first block to improve the estimation of vertical forces. Then two block are combined to estimate the tire forces. With a linear model, the vertical forces are estimated with Kalman Filter shown as below.

### A. Discrete-time State-space Representation

To build a Kalman Filter, the vertical force system has been represented by a set of discrete state-space equations:

$$\begin{aligned} x_k &= Ax_{k-1} + Bu_{k-1} + \omega_{k-1} \\ y_k &= Hx_k + v_k \end{aligned} \quad (12)$$

Where A is the states evolution matrix, H is the observation matrix. and  $\omega_k$   $v_k$  are white noises. Here, the vehicle state vector  $X \in R^{14}$  is defined as follows:

$$X = [ \phi \ \dot{\phi} \ \theta \ \dot{\theta} \ F_{z11} \ F_{z12} \ F_{z21} \ F_{z22} \ a_{xr} \ \dot{a}_{xr} \ a_{yr} \ \dot{a}_{yr} \ a_{zr} \ \dot{a}_{zr} ]^T \quad (13)$$

The initial value of X is:

$$X_0 = [0 \ 0 \ 0 \ 0 \ \frac{m_v g}{4} \ \frac{m_v g}{4} \ \frac{m_v g}{4} \ \frac{m_v g}{4} \ 0 \ 0 \ 0 \ 0 \ 0 \ 0]^T \quad (14)$$

In addition, the following assumption is made  $\ddot{a}_x = \ddot{a}_{ym} = \ddot{a}_{zr} = 0$ .

The continuous-time state equations are presented in equations (15). By discretizing the state equations we can obtain the evolution matrix A. And B=0.

$$\dot{X} = \begin{cases} \dot{\phi} = \dot{\phi} \\ \ddot{\phi} = \frac{m_v h}{I_{xx}} a_y - \frac{C_r}{I_{xx}} \dot{\phi} - \frac{K_r}{I_{xx}} \phi \\ \dot{\theta} = \dot{\theta} \\ \ddot{\theta} = \frac{m_v h}{I_{yy}} a_x - \frac{C_r}{I_{yy}} \dot{\theta} - \frac{K_r}{I_{yy}} \theta \\ \dot{F}_{z11} = \frac{m_v l_2}{2l} \dot{a}_{zr} - \frac{K_r \theta + C_r \dot{\theta}}{E_1} + \frac{K_r \phi + C_r \dot{\phi}}{l} \\ \dot{F}_{z12} = \frac{m_v l_2}{2l} \dot{a}_{zr} + \frac{K_r \theta + C_r \dot{\theta}}{E_1} + \frac{K_r \phi + C_r \dot{\phi}}{l} \\ \dot{F}_{z21} = \frac{m_v l_1}{2l} \dot{a}_{zr} - \frac{K_r \theta + C_r \dot{\theta}}{E_2} - \frac{K_r \phi + C_r \dot{\phi}}{l} \\ \dot{F}_{z22} = \frac{m_v l_1}{2l} \dot{a}_{zr} + \frac{K_r \theta + C_r \dot{\theta}}{E_2} - \frac{K_r \phi + C_r \dot{\phi}}{l} \\ \dot{a}_x = \dot{a}_x \\ \ddot{a}_x = 0 \\ \dot{a}_y = \dot{a}_y \\ \ddot{a}_y = 0 \\ \dot{a}_{zr} = \dot{a}_{zr} \\ \ddot{a}_{zr} = 0 \end{cases} \quad (15)$$

The observation model is linear and the output vector  $Y$  is presented as follows:

$$Y = [ \phi \dot{\phi} \theta \dot{\theta} F_{z11} F_{z12} F_{z21} F_{z22} a_{xr} a_{yr} a_{zr} ]^T \quad (16)$$

The elements in this vector are respectively provided by:

- $\phi, \theta$  are calculated by equation (7):
- $\dot{\phi}, \dot{\theta}$  is measured by the accelerometer
- $a_{xm}, a_{ym}, a_{zm}$  are measured directly from the accelerometer

Therefore, the observer matrix  $H$  can be simply determined by

$$Y = H * X \quad (17)$$

For our developed Kalman filter, the error measurement covariance is determined by the sensor variance, and the error model covariance is determined by the model quality.

Before applying the Kalman filter, we need to check observability of the system. Observability tells how well the internal states of a system can be inferred by the knowledge of the inputs and outputs. The observability matrix can be calculated by:

$$O = [ H \quad HA \quad HA^2 \quad \dots \quad HA^{n-1} ]^T \quad (18)$$

In our case, the observability matrix has full rank 14, therefore our system is observable.

#### IV. EXPERIMENTAL VALIDATION

As we have introduced in the abstract, both simulation software and experimental cars are used to evaluate the performance of the new observer. The performance of the developed observers was characterized by the normalized mean. The normalized error is defined in Stephant [8] as:

$$\varepsilon_z = 100 * \frac{|Z_{obs} - Z_{measure}|}{\max(|Z_{measure}|)} \quad (19)$$

where  $Z_{obs}$  is the value calculate by the observer,  $Z_{measure}$  is the measured value and  $(|Z_{measure}|)$  is the absolute maximum value of the measured data.

The new observer is designed to have a better performance in both banked road and inclined road. The object of our experiments is to testify this improvement. Therefore, all our tests are conducted in the condition of non-zero road angle.

In the simulation part, two Chicane tests have been done. One Chicane test is done with banked road. The bank angle of the road is 30%. The other test is done with inclined road. The incline angle is 20%. The velocity of the vehicle is about 30 km/h. The lateral acceleration is around (-0.5 g, 0.5g). The test lasts for about 20 second. The trajectory of this test is shown in Figure 6:

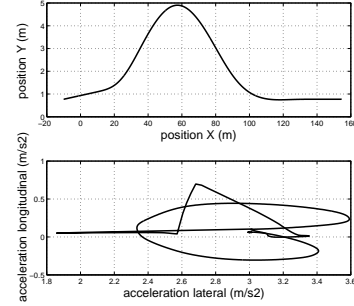


Fig. 6. Vehicle trajectory and acceleration

To verify the performance improvement, we also test the previous observer in the same condition to make a comparison.

#### A. Simulation of Chicane test at inclined road

This objective of the following simulation is to test our observer in inclined roads. The inclination angle is set as 20%. The observed vertical forces from the observers are shown in the following Figure 7. Simulation data of Callas are shown in red. The estimated values of the new observers are shown in dashed blue. The black dashed lines represent the observed values with the previous model.

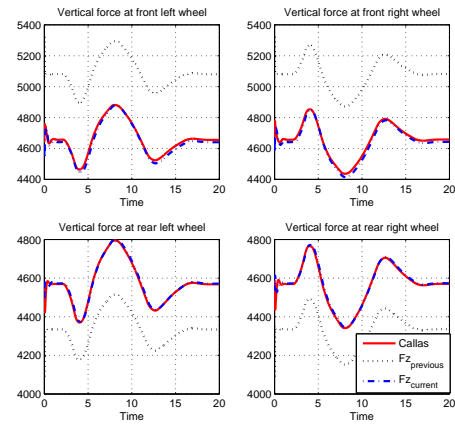


Fig. 7. Vertical Forces Estimation of each wheel at inclined road

The normalized mean error of the vertical forces estimation is shown in Table 1:

TABLE I  
ERROR OF VERTICAL FORCES ESTIMATION AT  
INCLINED ROAD

Error (%)	Fz11	Fz12	Fz21	Fz22
CurrentObserver	0.34	0.34	0.13	0.15
PreviousObserver	8.68	8.74	4.90	4.90

From the Table 1, we can see that the error of the new observer is less than 1%, while the previous observer has an error about 8%. In the new observer, we considered the component of gravity into the longitudinal dynamics, which makes the observer reliable even at inclined road.

### B. Simulation of Chicane test at banked road

The following simulation is to evaluate our observer at banked road. The bank angle is set as 30%. The observed vertical forces from the observers are:

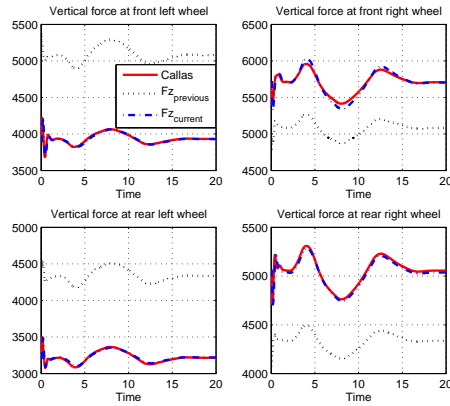


Fig. 8. Vertical Forces Estimation of each wheel at banked road

In Figure 8, the red lines represent Callas simulation data. The red lines data shows that vertical forces of right wheels are generally bigger than those of left wheels. That is correspondent to the bank angle. However, in the previous observer, presented by black dashed lines, the bank angle is not considered, so its observed values at right and left wheels are very similar. In contrast, with our current observer, the estimated value are very satisfactory. To evaluate the performance of both observers more precisely, the normalized mean error of the estimation is calculated:

TABLE II  
ERROR OF VERTICAL FORCES ESTIMATION AT BANKED  
ROAD

Error (%)	Fz11	Fz12	Fz21	Fz22
CurrentObserver	0.24	0.46	0.30	0.42
PreviousObserver	27.22	10.46	31.97	13.52

From the Table 2, we can see that the new observer has also a good performance in banked road. These good results confirm that the presented algorithm is suitable for estimation of vertical forces in banked road and inclined road.

### C. Experiments in real condition

After the validation of our observer by simulation, we use the experiment car to evaluate its performance in real condition. During the test, the experiment car was conduit on the city roads near our research center. The test takes 450 seconds and the total distance is about 6 km. Globally, all the real data is approach to our estimation. However, to present our experimental results more clearly, we choose only 80 seconds of the experimental data to analyze. Figure 9 shows the experimental car's trajectory, altitude, steering wheel angle and speed during this period of 80 seconds.

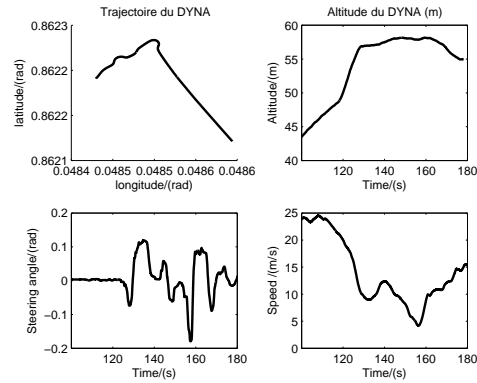


Fig. 9. Trajectory and altitude of experiment car during test

This data is chosen, because during the 80 seconds, the experimental car has experienced most driving situation we could meet in real condition. In the first 30 seconds, the car DYNA is climbing at the inclined road. Then it meets a sudden turning, as we can see in figure 9 in the trajectory of DYNA. After that, DYNA follows S-curve, which causes a sharp variation in steering wheel angle. The road condition is very complicated. To have correct estimation of vehicle dynamics requires the observer to maintain reliable regardless of the inclined road and banked road. The following figures show the results of our estimation.

The observed vertical forces from the observers are:

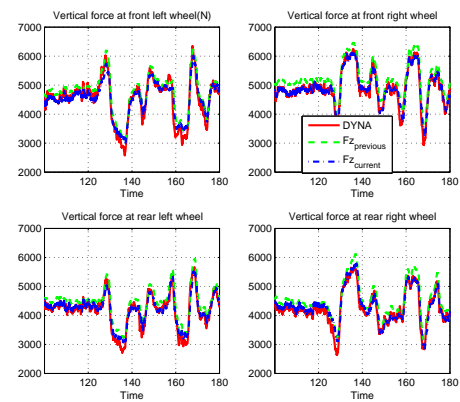


Fig. 10. Vertical Forces Estimation of each wheel in real road experiment

The red lines represent the measured value. We can see the vertical forces has underwent big variation during the experiment. That is caused by the road angle and turning behavior of the vehicle. The blue lines represent the estimated values by new observer. The green lines represent the previous observer. We can see the estimated values by the new observer are very close to the true value, which could validate our new vertical force model.

To evaluate the performance more precisely, the normalized mean error of the observer output is:

TABLE III  
VERTICAL FORCES ESTIMATION IN REAL CONDITION

Error (%)	Fz11	Fz12	Fz21	Fz22
Current Observer	2.49	1.63	1.94	2.05
PreviousObserver	3.40	4.52	4.10	4.60

With the observer structure shown in Figure 5, besides the vertical forces, our observer could also estimate lateral forces. Since the vertical forces estimation at banked road is improved, the observer of lateral forces is supposed to also have a good performance at banked road. To justify this suppose, we also measured the values of lateral forces in the real tests to evaluate the observer. The observed lateral forces from the observers are in the Figure 11:

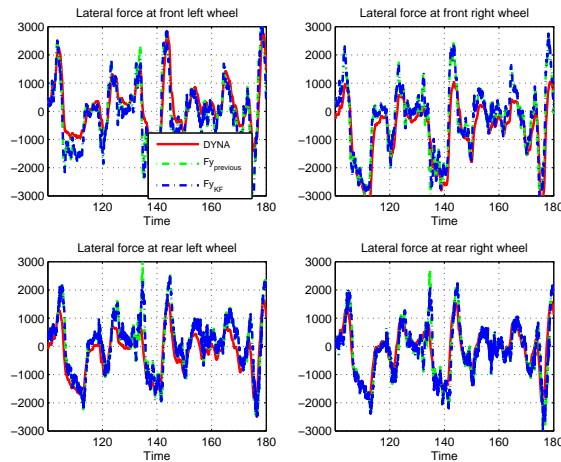


Fig. 11. Lateral Forces Estimation of each wheel in real road experiment

The estimated values of lateral forces are also very close to the reference data. The normalized mean error of the observer output is:

TABLE IV  
LATERAL FORCES ESTIMATION IN REAL CONDITION

Error (%)	Fy11	Fy11	Fy11	Fy11
Current Observer	6.04	6.69	6.10	6.31
PreviousObserver	6.05	6.72	6.21	6.42

## V. CONCLUSIONS AND PROSPECTS

This paper has presented a new model to estimate vertical tire forces. By distinguishing the acceleration caused by gravity and movement, the model can take in account the road angle and road irregularity. And in contrast to the previous model, the current model has considered the pitch dynamics and roll dynamics of the suspension. In conclusion, in our renovated model, pitch and roll dynamics and road disturbance are considered. Then combined with the lateral forces model in previous work and Kalman filter, we have developed observers to estimate the vertical and lateral tire forces of vehicle. Experiments have been made by both simulation software and real experimental car. Experimental results are presented to evaluate the performance of the new observer. Several critical tests are performed to compare and validate our new algorithm, The observer gives convenient results even when the car follows a S-curve on the inclined road.

However, the new observer works only when the vehicle physic parameters are already known and remain constant. Actually, some parameters considered as constant are changing during the driving process. To improve the precision of the observer, we should know exactly the physic parameters of vehicle, like position of center of gravity, the cornering stiffness, the suspension stiffness and so on. Future study will be concentrated at the estimation of these vehicle physic parameters.

## REFERENCES

- [1] B. Wang, A. C. Victorino and A. Charara, "State observers applied to vehicle lateral dynamics estimation: a comparison between Extended Kalman filter and Particle filter", 39th Annual Conference of the IEEE Industrial Electronics Society, Austria, Nov, 2013.
- [2] Baffet, G., et al. "Experimental evaluation of observers for tire-road forces, sideslip angle and wheel cornering stiffness." *Vehicle System Dynamics* 46.6 (2008): 501-520.
- [3] Baffet, Guillaume, Ali Charara, and Gerald Dherbomez. "An Observer of Tire-Road Forces and Friction for Active Security Vehicle Systems." *Mechatronics, IEEE/ASME Transactions on* 12.6 (2007): 651-661.
- [4] Doumiati, Moustapha, et al. "An estimation process for vehicle wheel-ground contact normal forces." *IFAC WC* 8 (2008).
- [5] Doumiati Moustapha. "Embedded estimation of vehicle's vertical and lateral tire forces for behavior diagnosis on the road." *Dissertation, University of Technology of Compiègne, 2009*
- [6] Kienecke, U., and Lars Nielsen. "Automotive control systems." Warrendale, PA: Society of Automotive Engineers, 2000. 432 (2000).
- [7] Shim, Taehyun, and Chinar Ghike. "Understanding the limitations of different vehicle models for roll dynamics studies." *Vehicle system dynamics* 45.3 (2007): 191-216.
- [8] J. Stéphant. *Contribution à l'étude et à la validation expérimentale d'observateurs appliqués à la dynamique du véhicule.* PhD thesis, Université de Technologie de Compiègne, 2004
- [9] Ryu, Jihan, and J. Christian Gerdes. "Estimation of vehicle roll and road bank angle." *American Control Conference, 2004. Proceedings of the 2004. Vol. 3. IEEE, 2004.*
- [10] Aleksander, H., Brown, T. & Martens, J. (2004). Detection of vehicle rollover, *Proceedings of the SAE World congress, Michigan, USA.*
- [11] A. Hac, T. Brown and J. Martens. *Detection of vehicle rollover. Vehicle Dynamics & Simulation, 2004.*
- [12] Doumiati, Moustapha, et al. "Unscented Kalman filter for real-time vehicle lateral tire forces and sideslip angle estimation." *Intelligent Vehicles Symposium, 2009 IEEE. IEEE, 2009.*
- [13] D. L. Milliken, E. M. Kasprak, L. Daniel Metz and W. F. Milliken. *Race car vehicle dynamics.* SAE International, 2003.